
Hepatic Hemangiomas: Evaluation by Magnetic Resonance Imaging and Technetium-99m Red Blood Cell Scintigraphy

Richard K.J. Brown,* Antoinette Gomes, William King, Elizabeth Pusey, Juan Lois, Leonard Goldstein, Ronald W. Busuttil, and Randall A. Hawkins

Division of Nuclear Medicine & Biophysics, Department of Radiological Sciences; Department of Medicine, Department of Surgery, UCLA School of Medicine; and Laboratory of Nuclear Medicine, Laboratory of Biomedical and Environmental Sciences, University of California, Los Angeles, California

A study was performed to evaluate and compare the sensitivity of magnetic resonance imaging (MRI) and radionuclide blood-pool scanning in the detection of hepatic hemangiomas. All patients had known hemangiomas which were first detected on either ultrasound or computed tomography. Sixteen patients with a total of 23 lesions were investigated. Eleven patients had both MRI and blood-pool scans performed. In the group studied by both modalities, 18 lesions were detected ranging in size from 1 to 11 cm. All lesions were detected by both techniques. However, two of the 18 lesions had an atypical appearance on MRI. Our experience to date indicates that the anatomic location and specific diagnosis of hemangiomas can be made with a high degree of certainty when both MRI and blood-pool scanning techniques are utilized.

J Nucl Med 28:1683-1687, 1987

Cavernous hemangiomas are the most common benign liver tumors. Autopsy studies report an incidence ranging from 0.4% to 7.3%. These lesions often present a clinical dilemma when they are first detected because they can simulate metastatic disease. Dynamic computed tomography (CT) scanning, angiography, and biopsy can usually establish the diagnosis with certainty. However, these procedures are not without risks. Previous reports have separately described the use of radionuclide pool scanning (RBPS) and magnetic resonance imaging (MRI) in the diagnosis of hemangiomas with impressive results. The classic finding on RBPS is an area of increased activity on the 2-hr delayed images. On MRI studies hepatic hemangiomas characteristically appear on T₁ weighted images as a low signal

or isobright mass which becomes homogeneously bright on the T₂ sequences (1-5). A study was performed in order to evaluate and compare the sensitivity of MRI and RBPS in the diagnosis of hepatic hemangiomas.

MATERIALS AND METHODS

Sixteen patients with a total of 23 lesions were investigated. The patients ranged in age from 35 to 68 yr old. There were 15 females and one male. RBPS studies were performed on all patients.

All patients studied had known hemangiomas which were first detected on either ultrasound or CT. The diagnosis was confirmed by angiography in four cases, biopsy in three cases, and long-term follow-up (2 or more years) with ultrasound in nine cases.

Eleven patients had both MRI and RBPS scans. In the group studied with both modalities 18 lesions ranging 1-11 cm in size were detected. In three of these cases pathologic confirmation of the lesions was obtained surgically.

RBPS studies were performed utilizing technetium-99m (^{99m}Tc) pertechnetate-labeled red blood cells ([Tc]RBCs). Ten cubic centimeters of the patient's blood was obtained and

Received Apr. 7, 1986; revision accepted May 20, 1987.

For reprints contact: Randall A. Hawkins, MD, PhD, Div. of Nuclear Medicine and Biophysics, UCLA School of Medicine, Los Angeles, CA 90024.

*Present address: Dept. of Radiology, Crittenton Hospital, 1101 W. University Dr., Rochester, MI 48063.

labeled with 20 mCi of [^{99m}Tc] pertechnetate. The blood was then incubated for 30 min and then re-injected into the patient. Two hours later delayed "blood-pool" images were acquired in the anterior, posterior, right anterior oblique, left anterior oblique, and right lateral projections. A large field-of-view (LFOV) gamma camera with a low-energy, all purpose energy collimator was used. Each image was acquired for a total of 750,000 counts.

MRI scans were performed using a 0.3 Tesla permanent magnet system (Fonar B-3000). Both T_1 and T_2 weighted images were obtained in all cases. T_1 weighted axial sequences were acquired with TE-28 and TR-500 msec. This sequence yielded seven sections 7 mm thick at 1-cm intervals. The total scan time for this sequence was 8 min 30 sec using a 256×256 matrix and two averages.

T_2 weighted images in the axial projection were acquired with a TE of 56 msec and TR of 1,000 msec. Coronal T_2 weighted images (TE = 84 msec and TR = 2,000 msec) were obtained in three cases in which the lesion was felt to be more ideally portrayed in the coronal projection. Although both sets

of images were T_2 weighted, the TE-56 msec, TR-1000 msec sequence still contains a significant amount of T_1 information.

RESULTS

Twenty-three hemangiomas were detected in 16 patients with the radionuclide technique. All lesions which were discovered on CT or ultrasound were correctly identified on the scintigraphic blood pool images. Fourteen of the patients had solitary lesions, and two patients had multiple lesions.

In the 11 patients studied with both MRI and RBPS, 18 lesions were present. Both techniques detected all lesions. On the T_1 weighted sequence, four of the lesions were of slightly lower signal than normal and the remaining 14 were isobright. All 18 lesions had a greater signal intensity than normal liver on the T_2 weighted sequences.

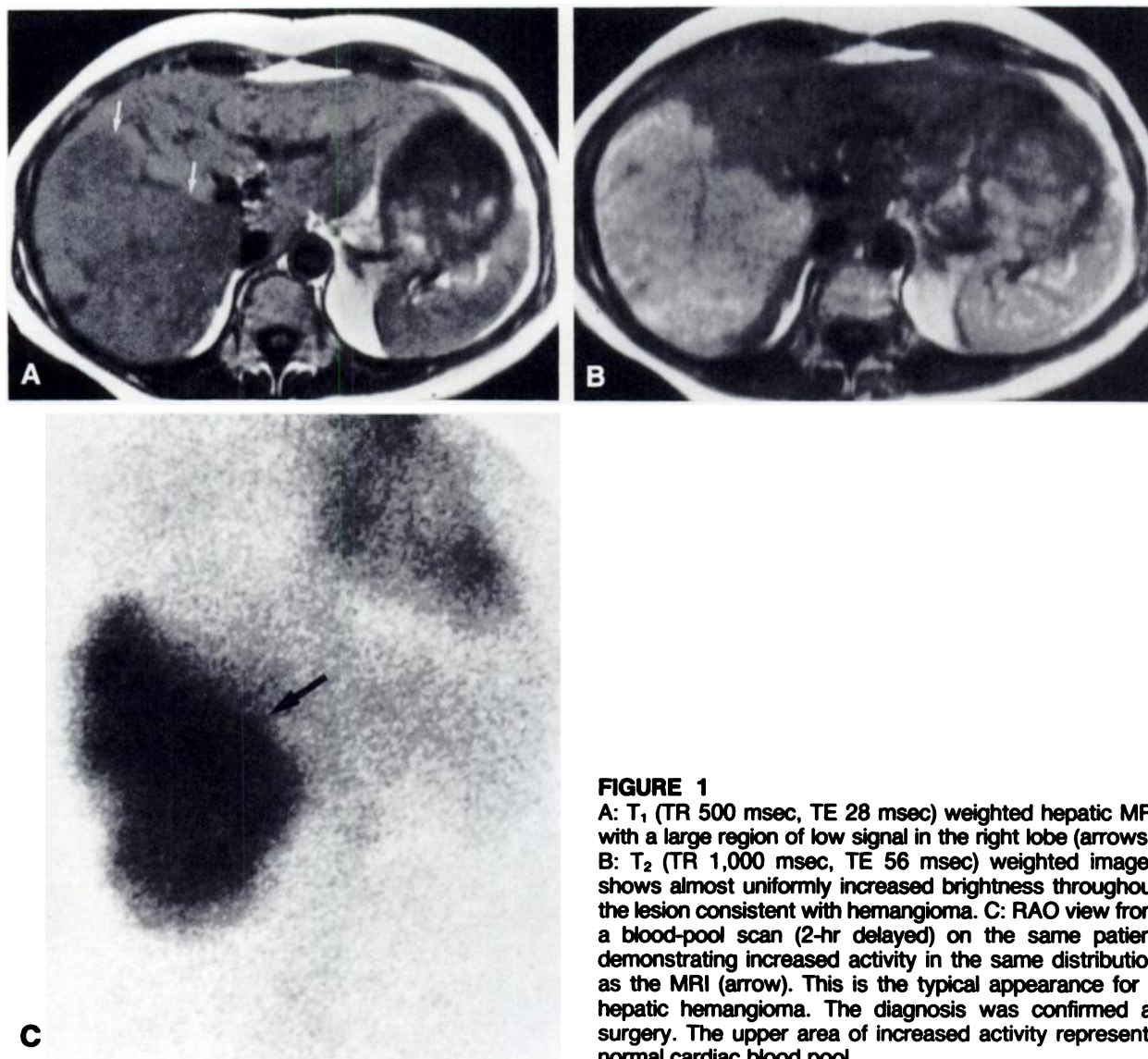


FIGURE 1

A: T_1 (TR 500 msec, TE 28 msec) weighted hepatic MRI with a large region of low signal in the right lobe (arrows). B: T_2 (TR 1,000 msec, TE 56 msec) weighted images shows almost uniformly increased brightness throughout the lesion consistent with hemangioma. C: RAO view from a blood-pool scan (2-hr delayed) on the same patient demonstrating increased activity in the same distribution as the MRI (arrow). This is the typical appearance for a hepatic hemangioma. The diagnosis was confirmed at surgery. The upper area of increased activity represents normal cardiac blood pool.

The classic appearance of a hepatic hemangioma was a well circumscribed lesion that was either isobright or demonstrated decreased brightness on the T₁ weighted images which on the T₂ weighted sequences lesions became homogeneously bright. Sixteen of the 18 lesions studied had the "classic" appearance on MRI. All but two of these 16 lesions demonstrated a lobulated contour. In these cases the ultrasound and CT studies also had characteristic features (Figs. 1 and 2). In one case the MRI demonstrated a mottled appearance on both the T₁ and T₂ sequences (Fig. 3). This lesion would not fit the criteria previously outlined for hemangiomas on MRI. The ultrasound in this case was also atypical. However, histologically the lesion was found to have

extensive fibrotic changes which may have contributed to the mottled signal. An additional case (not shown) of a surgically proven hemangioma also had an atypical MRI (mottled in homogeneous signal) probably as a result of recent hemorrhage in the lesion.

Twenty-two of the 23 lesions were studied by ultrasound. In all but two of these cases the ultrasound examination revealed findings typical of hemangiomas. These features included high echogenicity and well-circumscribed borders. In the other two cases the lesions had ill-defined sonographic borders. Five of the six lesions studied by CT were consistent with hemangiomas on the noncontrast and contrast study.

Since all 23 lesions were correctly identified and

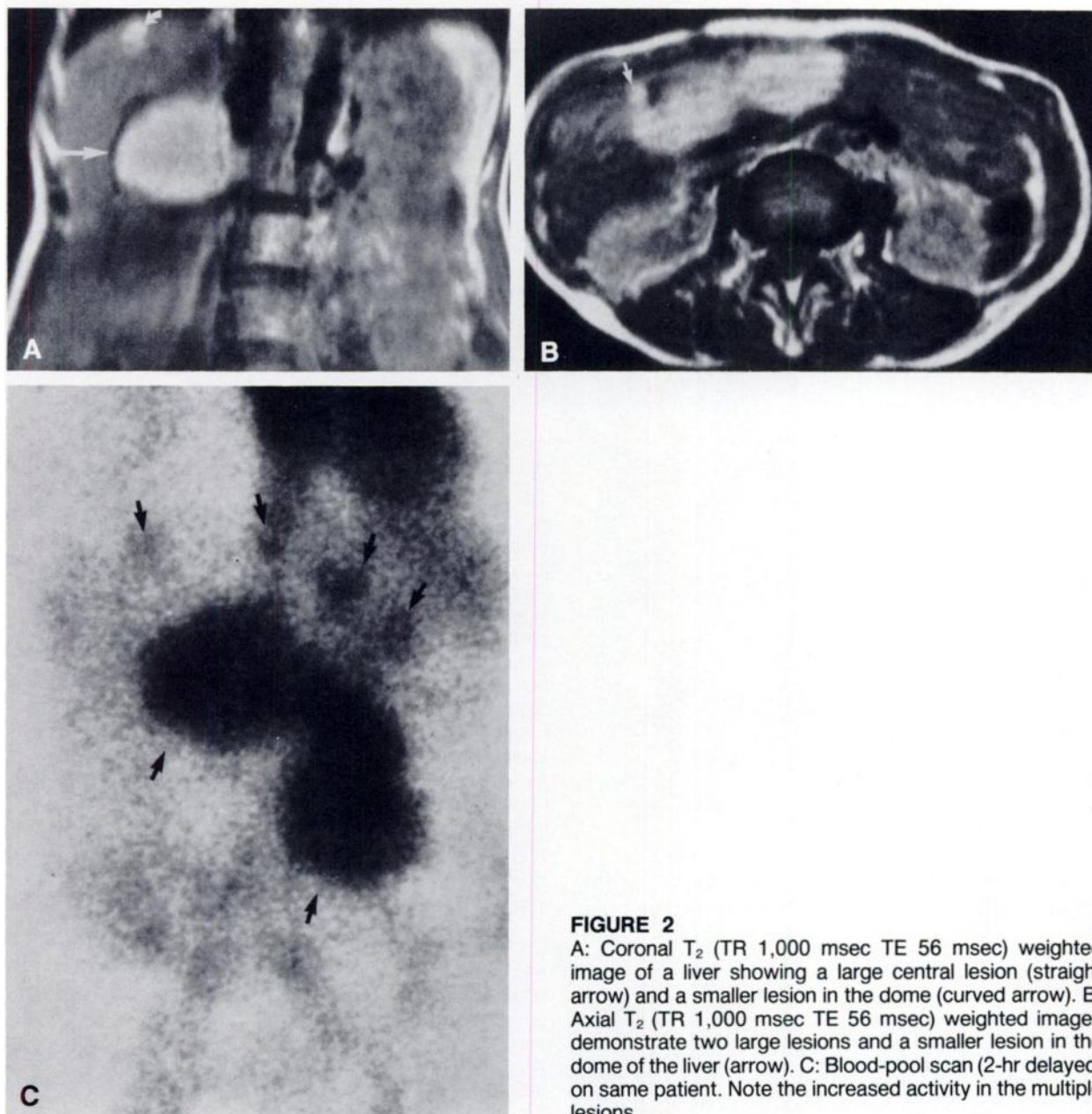


FIGURE 2
 A: Coronal T₂ (TR 1,000 msec TE 56 msec) weighted image of a liver showing a large central lesion (straight arrow) and a smaller lesion in the dome (curved arrow). B: Axial T₂ (TR 1,000 msec TE 56 msec) weighted images demonstrate two large lesions and a smaller lesion in the dome of the liver (arrow). C: Blood-pool scan (2-hr delayed) on same patient. Note the increased activity in the multiple lesions.

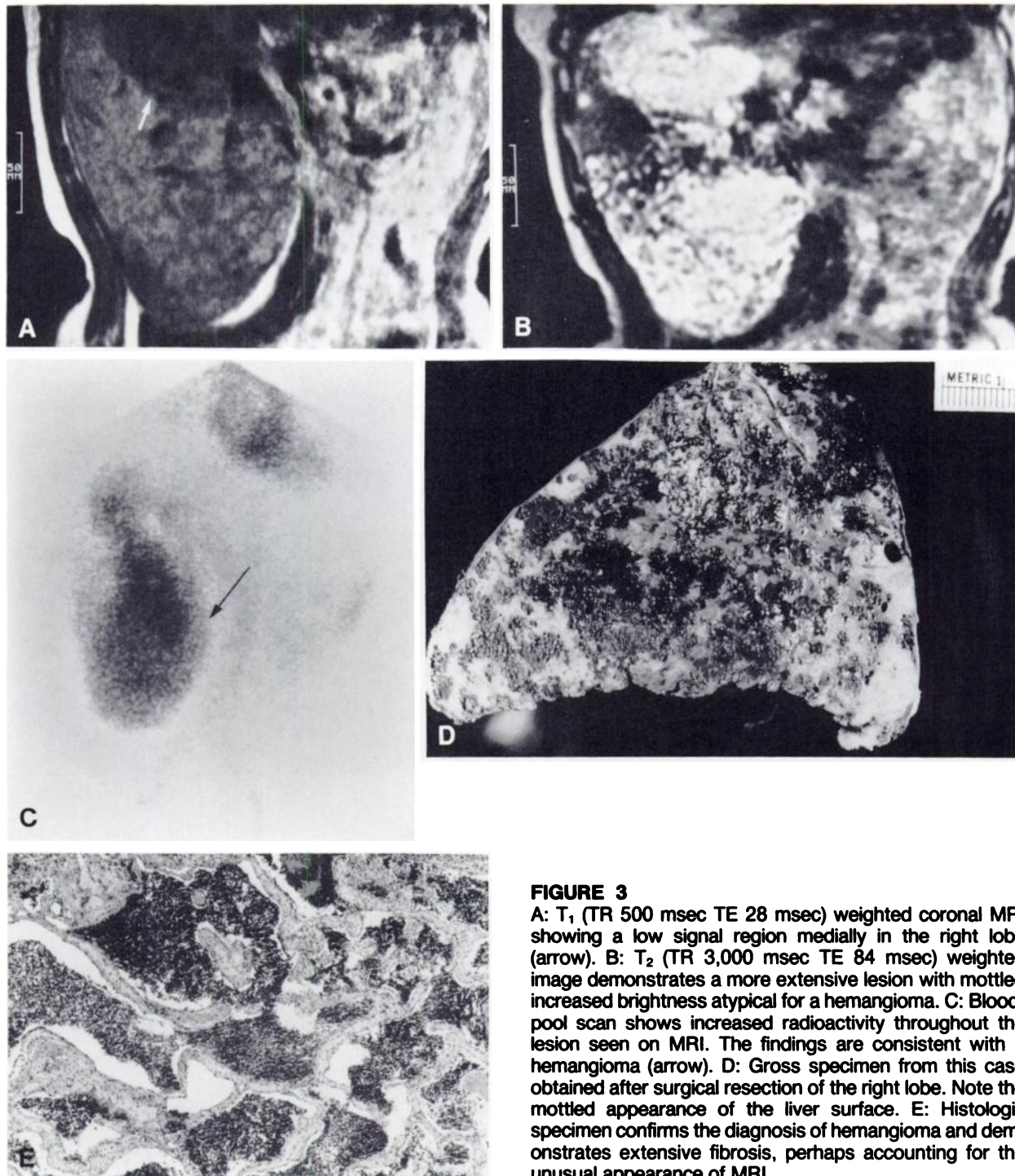


FIGURE 3

A: T₁ (TR 500 msec TE 28 msec) weighted coronal MRI showing a low signal region medially in the right lobe (arrow). B: T₂ (TR 3,000 msec TE 84 msec) weighted image demonstrates a more extensive lesion with mottled increased brightness atypical for a hemangioma. C: Blood-pool scan shows increased radioactivity throughout the lesion seen on MRI. The findings are consistent with a hemangioma (arrow). D: Gross specimen from this case obtained after surgical resection of the right lobe. Note the mottled appearance of the liver surface. E: Histologic specimen confirms the diagnosis of hemangioma and demonstrates extensive fibrosis, perhaps accounting for the unusual appearance of MRI.

characterized by the RBPS study the sensitivity of this test was 100%. All lesions were also identified on MRI.

DISCUSSION

Focal hepatic lesions are often discovered on both CT and ultrasound in asymptomatic patients. Hepatic hemangiomas should be ruled out when the liver func-

tion tests are normal or if there are features that suggest a benign lesion. Until recently, biopsy, angiography, and CT scanning with and without contrast enhancement were the most definitive methods for characterizing hemangiomas (6-11). All of these procedures are associated with some risk (12).

Both MRI and RBPS scanning have been proposed as alternative methods to characterize hepatic hemangiomas (13-15). In our series the radionuclide tech-

nique had a sensitivity of 100% and all cases had a characteristic appearance of increased uptake on delayed views. Using criteria described in the literature MRI also detected 100% of the lesions. The MRI technique demonstrated atypical characteristics in one large lesion with extensive fibrosis and in a second case which had recently hemorrhaged. These lesions demonstrate the wide range of appearances of hepatic hemangiomas on MRI.

Because of the high sensitivity and previously reported specificity of the RBPS technique a positive result should usually preclude further diagnostic evaluation.

Although both MRI and RBPS techniques are highly sensitive, the radionuclide technique may be more useful in lesions with extensive fibrosis or which have recently hemorrhaged.

Our experience to date indicates that the anatomic location and specific diagnosis of hepatic hemangioma can be made with a high degree of certainty when both MRI and blood-pool scanning techniques are combined. In cases where hepatic hemangiomas are suspected on the basis of the MRI on the anatomic imaging study, then blood-pool scanning should be the next diagnostic modality of choice.

ACKNOWLEDGMENTS

Operated for the U.S. Department of Energy by the University of California under Contract #DE-AC03-76-SF00012. This work was supported in part by the Director of the Office of Energy Research, Office of Health and Environmental Research, by NIH Grant NS 20867, NS 15654 and MH 37916.

REFERENCES

1. Stark DD, Felder RC, Wittenberg J, et al. Magnetic resonance imaging of cavernous hemangiomas of the liver: tissue-specific characterization. *Am J Roentgenol* 145:213-222.
2. Engel MA, Marks DS, Sandler MA, et al. Differentiation of focal intrahepatic lesions with ^{99m}Tc -red blood cell imaging. *Radiology* 1983; 146:777-782.
3. Rabinowitz SA, McKusick KA, Strauss HW. ^{99m}Tc red blood cell scintigraphy in evaluating focal liver lesions. *Am J Roentgenol* 1984; 143:63-68.
4. Glazer GM, Aisen AM, Francis IR, et al. Hepatic cavernous hemangioma: magnetic resonance imaging [Work in Progress]. *Radiology* 1985; 155:417-420.
5. Moinuddin M, Allison JR, Montgomery JH, et al. Scintigraphic diagnosis of hepatic hemangioma: its role in the management of hepatic mass lesions. *Am J Roentgenol* 145:223-228.
6. Barnett PH, Zerhouni EA, White RI Jr, et al. Computed tomography in the diagnosis of hemangioma of the liver. *Radiology* 1980; 137:149-155.
7. Freeny PC, Vimont TR, Barnett DC. Cavernous hemangioma of the liver: ultrasonography, arteriography, and computed tomography. *Radiology* 1979; 132:143-148.
8. Abrams RM, Beranbaum ER, Sants JS, et al. Angiographic features of cavernous hemangiomas of the liver. *Radiology* 1969; 92:308-312.
9. McLoughlin MJ. Angiography in cavernous hemangioma of the liver. *Am J Roentgenol* 1971; 113:50-55.
10. Johnson CM, Sheedy PF II, Stanson AW, et al. Computed tomography and angiography of cavernous hemangiomas of the liver. *Radiology* 1981; 138:115-121.
11. Ita Y, Furui S, Araki T, et al. Computed tomography of cavernous hemangioma of the liver. *Radiology* 1980; 137:149-155.
12. Kata M, Sugawara I, Okada A, et al. Hemangioma of the liver. Diagnosis with combined use of laparoscopy of hepatic arteriography. *Am J Surg* 1975; 129:698-704.
13. Glazer GM, Aisen AM, Francis IR, et al. Hepatic cavernous hemangioma: magnetic resonance imaging [Work in Progress]. *Radiology* 1985; 155:417-420.
14. Itai Y, Ohtomo K, Furui S, et al. Noninvasive diagnosis of small cavernous hemangioma of the liver: advantage of MRI. *Am J Roentgenol* 1985; 145:1195-1199.
15. Front D, Royal HD, Parker JA, et al. Scintigraphy of hepatic hemangiomas: the value of ^{99m}Tc -red blood cells: concise communication. *J Nucl Med* 1981; 22:684-687.